

# Design of a Robust Controller for a Magnetic Levitation System

Shafayet Hossain, Graduate Student (ECE), Wichita State University, Wichita, KS

**Abstract-** A Magnetic Levitation System (Maglev) is considered as a good test-bed for the design and analysis of control systems since it is a nonlinear unstable plant with practical uses in high-speed transportation and magnetic bearings. The objective of this project is to design a robust controller and implement it on a test-bed to help students learn the robust control design. In this project a robust controller for a maglev system is designed, using H-infinity optimization [3]. Complete mathematical models of the electrical, mechanical and magnetic systems are also developed. The design and simulations are performed under a Matlab/Simulink platform. Wincon control software of Quanser Inc. [7] is used to establish the link between the Matlab/Simulink models and the actual magnetic levitation system.

*Index Terms* – Robust control, stability and performance robustness.

## I. INTRODUCTION

Robust control explicitly deals with uncertainty in its approach to controller design. Controllers designed using robust control methods are able to cope with small differences between the actual system and the nominal model used for the design. This paper is focused on robust control analysis and design. The design and implementation issues of robust controllers and the use of H-infinity loop shaping method are addressed by using block diagrams and transfer functions along with Matlab/Simulink programs.

The paper is organized in different sections. In Section II, stability and performance

concepts for a typical control system structure are presented. Detailed description of a maglev system with mathematical models are provided in Section III. Step by step design procedures and H-infinity controller design are addressed in Section IV and V. In Section VI, simulations and laboratory results are analyzed. Concluding remarks are included in Section VII.

## II. STABILITY AND PERFORMANCE

A diagram of typical feedback control system is shown in Fig. 2.1. From Fig. 2.1 the following relations can be summarized:

$$r - y = Sr \quad (2.1)$$

$$y = Tr \quad (2.2)$$

$$u = KSr \quad (2.3)$$

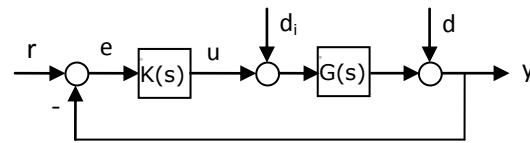


Fig. 2.1 Typical feedback control system

(2.1), (2.2) and (2.3) yield the feedback matrices from  $r$  to the outputs  $(r-y)$ ,  $y$  and  $u$  respectively. In Figure 2.1  $G(s)$  is the nominal plant and  $K(s)$  is the controller. The matrices  $S$  and  $T$  are referred to as sensitivity and complementary sensitivity matrices where

$$S(s) = (I + G(s)K(s))^{-1} \quad (2.4)$$

$$T(s) = G(s)K(s)(I + G(s)K(s))^{-1} \quad (2.5)$$

$$= I - (I + G(s)K(s))^{-1} = I - S(s) \quad (2.6)$$

Since (2.1) shows that  $e = r - y = Sr$ , the sensitivity matrix  $S$  determines the steady-state behavior of the feedback system. From

Fig. 2.1 we can show that  $y = Sd$  and  $y = SGd_i$ , which imply that the sensitivity matrix also determines the disturbance attenuation. Therefore, by specifying an upper bound on the norm of  $S(s)$  the disturbance attenuation and steady-state specifications can be addressed as follows:

$$|\bar{\sigma}(S(j\omega))| \leq |W_1^{-1}(j\omega)|, \quad \forall \omega \quad (2.7)$$

where  $\bar{\sigma}(S(j\omega))$  is the maximum singular value of  $S(s)$  and  $W_1$  is the bound that reflects the desired disturbance attenuation for each frequency  $\omega$ . Good disturbance rejection is required particularly in the low frequency region where disturbance is significant. From (2.3) the transfer function from input  $r$  to control  $u$  is given by  $R(s) = K(s)S(s)$ . Hence, constraint on the control  $u$  can be introduced with a bound  $W_2$  as shown by (2.8):

$$|\bar{\sigma}(K(j\omega)S(j\omega))| \leq |W_2^{-1}(j\omega)|, \quad \forall \omega \quad (2.8)$$

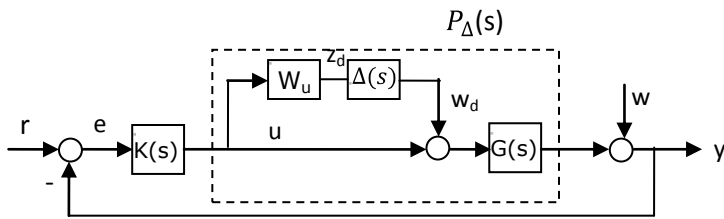


Fig. 2.2: Multiplicative unstructured uncertainty

Uncertainty in the mathematical model of the system is in general described as a perturbation to the nominal system. Unstructured uncertainty is only known in terms of its upper and lower bounds. When a detailed model of the uncertainty is known it is referred to as structured uncertainty. For a set of perturbations satisfying the infinity norm  $\|\Delta\|_\infty \leq 1$ , the perturbed plant can be modeled in terms of multiplicative unstructured uncertainty, with respect to the nominal plant  $G$ , as shown in Fig. 2.2 where

$$P_\Delta = G(I + \Delta_M) \quad (2.9)$$

where  $\Delta_M = W_u \Delta$

The frequency structure of the uncertainty is characterized by a stable transfer function  $W_u$ . In practical systems, a stability robustness test is needed, as in general, systems operate under perturbations. The system in Fig. 2.2 is stable if  $\Delta = 0$  the size of the smallest stable  $\Delta_M(s)$  for which the system becomes unstable is thus given by:

$$|\bar{\sigma}(\Delta_M(j\omega))| = \frac{1}{\bar{\sigma}(T(j\omega))} \quad (2.10)$$

Thus, the upper bound on  $\|T(s)\|_\infty$  can be specified as follows:

$$|\bar{\sigma}(T(j\omega))| \leq |W_3^{-1}(j\omega)|, \quad \forall \omega \quad (2.11)$$

Weighting function  $W_3$  is used to ensure good robustness and noise rejection, particularly in the high-frequency range where the noise and modeling errors are usually significant.

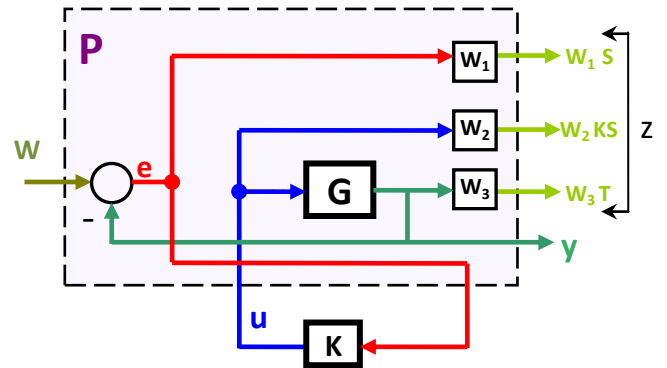


Fig. 2.3 : Augmented plant with weighting function

A typical interconnection model for design is illustrated in Fig. 2.3, where the weighting functions  $W_1, W_2, W_3$  reflect the specified steady-state error and the disturbance attenuation, controller input constraints and stability condition, respectively as evident from (2.7), (2.8) and (2.11).

The augmented plant of Fig. 2.3 has  $w$  and  $u$  as its inputs and  $z$  and  $y$  as outputs. The output  $z$  is the vector of regulated variables  $W_1S, W_2KS$  and  $W_3T$ .

The reference command  $r$  and error  $e = r - y$  of the typical feedback diagram of Fig. 2.1 correspond to  $w$  and  $y$  of Fig. 2.3. The input-output relationship of the system shown in Fig. 2.3 can be written as

$$\begin{bmatrix} z \\ y \end{bmatrix} = P \begin{bmatrix} w \\ u \end{bmatrix} = \begin{bmatrix} P_{11} & P_{12} \\ P_{21} & P_{22} \end{bmatrix} \begin{bmatrix} w \\ u \end{bmatrix} \quad (2.12)$$

$$\text{and } u = K(s) y \quad (2.13)$$

Putting the value of (2.13) in to (2.12), the closed-loop transfer matrix from  $w$  to  $z$  can be found as:

$$T_{zw} = P_{11} + P_{12} K (I - P_{22} K)^{-1} P_{21} \quad (2.14)$$

The mapping of (2.14) is known as a Linear Fractional Transformation (LFT), which is denoted by  $F_l(P, K)$  where the subscript 'l' indicates lower LFT.

A 3 block system is shown in Fig. 2.4 with an uncertainty block that should be considered to model general systems.

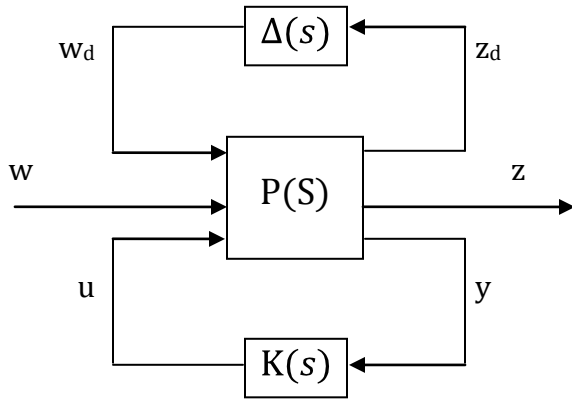


Fig. 2.4 : General block of model with uncertainty

Using the LFT,  $F_l(P, K)$ , the three-block system of Fig 2.4 can be reduced to the two-block M- $\Delta$  structure as shown in Fig. 2.5 :

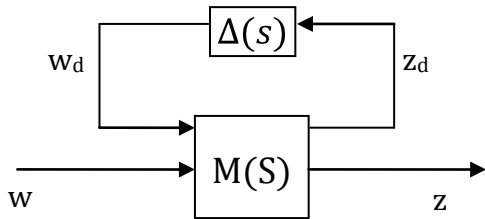


Fig. 2.5 : M-  $\Delta$  structure

$$\begin{bmatrix} z_d \\ z \end{bmatrix} = M \begin{bmatrix} w_d \\ w \end{bmatrix} = \begin{bmatrix} M_{11} & M_{12} \\ M_{21} & M_{22} \end{bmatrix} \begin{bmatrix} w_d \\ w \end{bmatrix} \quad (2.15)$$

$$w_d = \Delta z_d \quad (2.16)$$

Substituting (2.16) into (2.15)

$$z = F_u(M, \Delta) w$$

$$z = [M_{22} + M_{21} \Delta (I - M_{11} \Delta)^{-1} M_{12}] w \quad (2.17)$$

In (2.17) the subscript 'u' indicates upper LFT and the transfer matrix from the output vector  $z$  to reference or disturbance  $w$  is obtained as:  $T_{zw} = F_u(M, \Delta)$ .

### III. MAGNETIC LEVITATION SYSTEM

In this section, a physical maglev system and its components are described. Presenting system equations nonlinear and linear models are developed for the plant. The schematic of the MAGLEV plant is presented in Fig. 3.1 below:

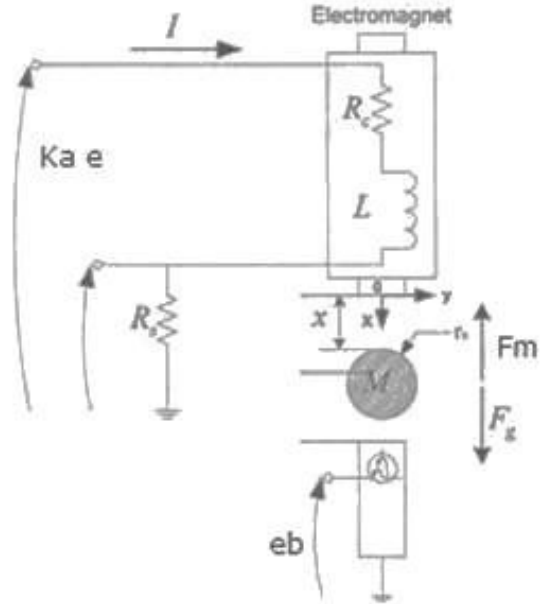


Fig. 3.1: Maglev system by Quanser [7]

As illustrated in Fig. 3.1, the positive direction of the vertical displacement is downwards with the origin of the global Cartesian frame of coordinates on the electromagnet core flat face. It can be seen

that maglev system consists of magnetic, electrical and mechanical systems.

### A. Magnetic System

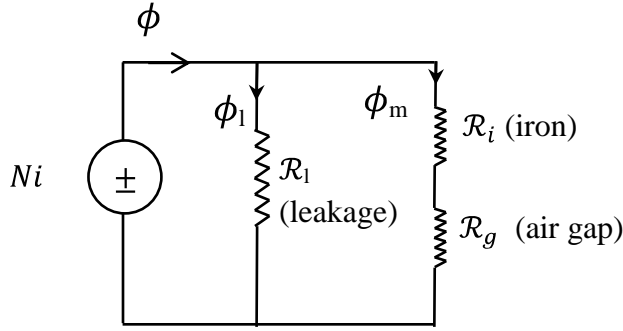


Fig. 3.2: Network for the electromagnet

From Fig.3.2

$$Ni = \Phi_l \mathcal{R}_l + \Phi_m (\mathcal{R}_i + \mathcal{R}_g) \quad (3.1)$$

Here,

$$\text{for iron path, } \mathcal{R}_i = \frac{l_i}{\mu_r \mu_0 A_i} = \frac{l_i}{\mu_r \mu_0 A_i}$$

$$\text{for air gap, } \mathcal{R}_g = \frac{2x}{\mu_0 A_i} = \frac{2x}{\mu_0 A_i}; \quad \mu_g \approx \mu_0$$

The magnetic flux

$$\phi_m = \frac{Ni}{\mathcal{R}_i + \mathcal{R}_g} = \frac{Ni}{\mathcal{R}_m} \quad \text{and} \quad \phi_l = \frac{Ni}{\mathcal{R}_l}$$

Total reluctance

$$\mathcal{R}_m(x) = (\mathcal{R}_i + \mathcal{R}_g) = \frac{l_i}{\mu_r \mu_0 A_i} + \frac{2x}{\mu_0 A_i}$$

$$\mathcal{R}_m(x) = \frac{1}{\mu_0 A_i} \left( \frac{l_i}{\mu_r} + 2x \right) \quad (3.2)$$

$$\phi = \phi_l + \phi_m = \frac{Ni}{\mathcal{R}_l} + \frac{Ni}{\mathcal{R}_m} \quad (3.3)$$

where,  $\phi_m$  = magnetic flux and  $\phi_l$  = leakage flux,  $\mathcal{R}_i$  = reluctance for iron path,  $\mathcal{R}_g$  = reluctance for air gap,  $l_i$  = mean length of iron path,  $A_i$  = area of the electromagnet surface,  $N$  = number of turns in the coil,  $i$  = coil current,  $\mu_0$  = permeability for free space,  $\mu_r$  = relative permeability of iron

### B. Electrical System

The electrical system is shown on Fig. 3.3. using KVL for the loop

$$k_a e = (R_c + R_s)i + \frac{d\lambda}{dt} = Ri + \frac{d\lambda}{dt} \quad (3.4)$$

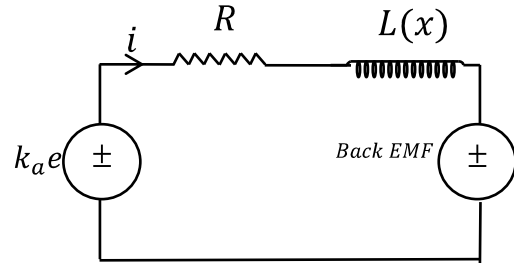
where  $k_a$  = power amplifier gain,  $e$  = actual coil input voltage,  $R_c$  = coil resistance,  $R_s$  = current sense resistance,  $R = (R_c + R_s)$ ,  $i$  = coil current and  $\lambda = N\phi$  which can be written as:

$$\lambda = N \left( \frac{N_i}{\mathcal{R}_l} + \frac{N_i}{\mathcal{R}_m(x)} \right)$$

$$\lambda = N \left( \frac{N^2}{\mathcal{R}_l} + \frac{N^2}{\mathcal{R}_m(x)} \right) i = (L_l + L_m(x)) i \quad (3.5)$$

$$\lambda(i, x) = L(x)i; \quad \text{where } L = \text{coil inductance}$$

$$L(x) = L_l + L_m(x)$$



≈

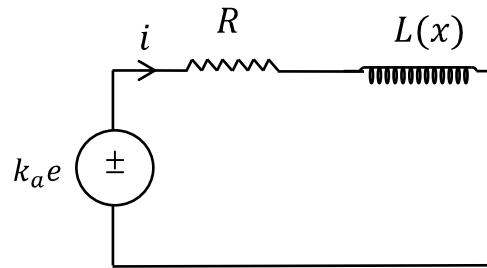


Fig. 3.3: Electrical model

The voltage drop due to the inductance

$$\frac{d\lambda}{dt} = \frac{\partial \lambda(i, x)}{\partial i} \frac{di}{dt} + \frac{\partial \lambda(i, x)}{\partial x} \frac{dx}{dt}$$

$$\frac{d\lambda}{dt} = L(x) \frac{di}{dt} + \frac{\partial L(x)}{\partial x} i \frac{dx}{dt} \quad (3.6)$$

$\frac{\partial L(x)}{\partial x} = \frac{\partial}{\partial x} L_m(x)$ ; without leakage inductance

$$L_m(x) = \frac{N^2}{R_m(x)} = \frac{N^2}{\frac{1}{\mu_0 A_i} \left( \frac{l_i}{\mu_r} + 2x \right)}$$

Rearranging the previous equation

$$L_m(x) = \frac{\frac{N^2 \mu_0 A_i}{2}}{\left( \frac{l_i}{2\mu_r} + x \right)}$$

$$L_m(x) = \frac{k}{(k_0 + x)} \approx \frac{k}{x} \text{ for } x \gg k_0 \quad (3.7)$$

where  $k = N^2 \mu_0 A_i / 2$ ;  $k_0 = \frac{l_i}{2\mu_r}$

$$\frac{\partial}{\partial x} L_m(x) = \frac{\partial}{\partial x} (k(k_0 + x)^{-1})$$

$$\frac{\partial}{\partial x} L_m(x) = -\frac{k}{(k_0 + x)^2} \quad (3.8)$$

Using (3.6), (3.4) can be written as:

$$k_a e = Ri + \frac{d}{dt} (L(x)i) + \frac{\partial L(x)}{\partial x} i \frac{dx}{dt}$$

where  $\frac{\partial L(x)}{\partial x} i \frac{dx}{dt}$  = counter electromotive force or back emf produced by the changing electromotive force.

$$k_a e = Ri + L(x) \frac{di}{dt} - \frac{K}{(K_0 + x)^2} i \frac{dx}{dt} \quad (3.9)$$

As the leakage flux in this case is very low therefore the back emf can be ignored from (3.9) and can be written as:

$$k_a e = Ri + L(x) \frac{di}{dt} \quad (3.10)$$

### C. Mechanical System

Energy stored in the inductor can be written as:  $W_e = \frac{1}{2} L(x) i^2$  (3.11)

Power in the electrical system  $P_e$  = Power in the mechanical system  $P_m$

where  $P_e = \frac{dW_e}{dt}$  and  $P_m = -f_m \frac{dx}{dt}$

As  $P_e = P_m$  therefore,

$$-f_m \frac{dx}{dt} = \frac{dW_e}{dt}$$

$$f_m = -\frac{dW_e}{dt} \frac{dt}{dx} = -\frac{dW_e}{dx}$$

Substituting (3.11) in the above equation

$$f_m = -\frac{d}{dx} \left( \frac{1}{2} L(x) i^2 \right)$$

$$f_m = -\frac{1}{2} i^2 \frac{d}{dx} (L(x)) = -\frac{1}{2} i^2 \left( \frac{-k}{x^2} \right)$$

$$f_m = \frac{k}{2} \left( \frac{i^2}{x^2} \right) \quad (3.12)$$

where k = electromagnet force constant, x = actual air gap between core face and ball surface,  $P_e$  = power in the electrical system,  $P_m$  = power in the mechanical system,  $f_m$  = electromagnet force,

Therefore the equation of force can be written as:  $f_g = f_m + f$

$f = M \left( \frac{d^2 x}{dt^2} \right)$  = resultant force and  $f_g$  = force due to gravity

$$M \left( \frac{d^2 x}{dt^2} \right) = -f_m + f_g$$

$$\left( \frac{d^2 x}{dt^2} \right) = -\frac{1}{M} f_m + \frac{1}{M} f_g = \frac{dv}{dt} \quad (3.13)$$

where M = steel ball mass and  $v = \frac{dx}{dt}$  = velocity of the ball movement

At equilibrium:  $f_g = -f_m$  and  $f = 0$

### Model Summary:

Magnetic:  
The reluctance due to the inductor

$$R_m(x) = \frac{1}{\mu_0 A_i} \left( \frac{l_i}{\mu_r} + 2x \right) \quad (3.14)$$

Electrical:

$$k_a e = Ri + L(x) \frac{di}{dt} \quad (3.15)$$

Mechanical:

$$M \left( \frac{dv}{dt} \right) = -f_m(x, i) + f_g \text{ and } v = \frac{dx}{dt} \quad (3.16)$$

$$f_m(x, i) = -\frac{1}{2} i^2 \frac{d}{dx} (L(x)) = \frac{k}{2} \left( \frac{i^2}{x^2} \right) \quad (3.17)$$

#### D. Non-Linear Model

$$\frac{di}{dt} = \frac{1}{L(x)} [k_a e(t) - Ri] \quad (3.18)$$

$$\frac{dx}{dt} = v \text{ and } \frac{dv}{dt} = \frac{1}{M} (-f_m(x, i)) \quad (3.19)$$

#### E. Linear Model

The states of the system are  $i$ ,  $v$  and  $x$ . At equilibrium the force due to gravity  $f_g$  and the magnetic force  $f_m$  are equal and opposes each other so the ball levitates. Considering, nominal input voltage  $e_0$  produces the corresponding coil current  $i_0$  such that the ball reaches at its equilibrium where position  $x = x_0$ , it can be linearized using Taylor's expansion around the equilibrium  $(x_0, i_0)$ , where  $x = x_0 + \Delta x$  and  $i = i_0 + \Delta i$ , then the magnetic force is:

$$f_m(x, i) \cong f_m(x_0, i_0) + \left. \frac{\partial f_m}{\partial x} \right|_{(x_0, i_0)} \Delta x + \left. \frac{\partial f_m}{\partial i} \right|_{(x_0, i_0)} \Delta i \quad (3.20)$$

$$f_m \cong f_{m0} - k_s \Delta x + k_i \Delta i \quad (3.21)$$

where  $f_m(x, i) = f_m$  and  $f_m(x_0, i_0) = f_{m0}$

$$k_s = - \left. \frac{\partial f_m}{\partial x} \right|_{(x_0, i_0)} = k \left( \frac{i_0^2}{x_0^3} \right)$$

$$k_i = \left. \frac{\partial f_m}{\partial i} \right|_{(x_0, i_0)} = k \left( \frac{i_0}{x_0^2} \right)$$

Now the governing equations can be written as:

$$L(0) \frac{d}{dt} \Delta i + R \Delta i = k_a \Delta e \quad (3.22)$$

$$M \left( \frac{dv}{dt} \right) - k_s \Delta x + k_i \Delta i = 0 \quad (3.23)$$

$$\frac{d}{dt} \Delta x = v \quad (3.24)$$

From (3.22), (3.23) and (3.24)

$$\frac{d}{dt} \begin{bmatrix} \Delta i \\ v \\ \Delta x \end{bmatrix} = \begin{bmatrix} -\frac{R}{L} & 0 & 0 \\ -\frac{k_i}{M} & 0 & \frac{k_s}{M} \\ 0 & 1 & 0 \end{bmatrix} \begin{bmatrix} \Delta i \\ v \\ \Delta x \end{bmatrix} + \begin{bmatrix} \frac{k_a}{L} \\ 0 \\ 0 \end{bmatrix} \Delta e \quad (3.25)$$

(3.25) can be written in the form of state space as (3.26)

$$\dot{X} = A X + B u \text{ and } Y = C X + D u \quad (3.26)$$

where  $A$  =state matrix,  $B$  =input matrix,  $C$  =output matrix and  $D$  = feed through (feed forward ) matrix.

Comparing (3.25) and (3.26)  $A$ ,  $B$ ,  $C$  and  $D$  matrices for the linear maglev model can be written as:

$$A = \begin{bmatrix} -\frac{R}{L} & 0 & 0 \\ -\frac{k_i}{M} & 0 & \frac{k_s}{M} \\ 0 & 1 & 0 \end{bmatrix}; \quad B = \begin{bmatrix} \frac{k_a}{L} \\ 0 \\ 0 \end{bmatrix};$$

$$C = (0 \ 0 \ 1) \text{ and } D = 0$$

## IV. DESIGN PROCEDURE

### Weighting Functions

For a specific design problem the selection of the weighting functions is an involved task. The requirements for the selection of weighting functions are discussed in Stability and Robustness Section. After extensive simulation and fine tuning, the weighting function  $W_1$  for the sensitivity  $S$ ,  $W_2$  for  $KS$  and  $W_3$  for complementary sensitivity  $T$  are chosen as follows:

$$W_1 = \frac{0.89023 (s + 1.123)}{(s + 1.006)}$$

$$W_2 = 1e^{-8}$$

$$W_3 = \frac{0.3548 (s + 49.14)}{(s + 39.03)}$$

The function  $W_1$  is the bound for the sensitivity function and reflects external

disturbance rejection, a small steady-state error with respect to the desired equilibrium, and plant variations tolerance, i.e, the performance specifications.  $W_2$  weights KS reflecting the control input constraints. The function  $W_3$  satisfies the peak requirement on the complementary sensitivity function T to reduce the system oscillations and to limit T in the high-frequency range for stability.

#### Parameter Uncertainty

Considering the case of high speed transportation systems a 10% variation of mass is included as parameter uncertainty. This variation can be written as:

$M=M+ 0.1\delta M$ , where  $M$  = mass of the steel ball and  $-1 \leq \delta \leq 1$ . The term  $1/M$  can further be written as:

$$\frac{1}{M} = \frac{1}{M} - \frac{0.1\delta}{M} (1 + 0.1\delta)^{-1} \quad (4.1)$$

Comparing (4.1) with (2.16) the LFT matrix  $M_1$  can be found as [2]:

$$M_1 = \begin{bmatrix} -0.1 & 1 \\ -0.1 & 1 \\ \frac{1}{M} & \frac{1}{M} \end{bmatrix}$$

This LFT can be represented as:

$$F_u \left( \delta, \begin{bmatrix} -0.1 & 1 \\ -0.1 & 1 \\ \frac{1}{M} & \frac{1}{M} \end{bmatrix} \right)$$

Initially, changing 10% of mass in the matlab simulation the bound for the weight  $W_3$  was chosen to weight the complementary sensitivity function, T.

#### V. $H_\infty$ CONTROLLER DESIGN

The standard  $H_\infty$  optimal control problem is to find all stabilizing controllers K that satisfy

$$\|T_{zw}\|_\infty = \|[W_1S \ W_2KS \ W_3T]^T\|_\infty \leq \gamma \quad (5.1)$$

where  $\gamma < 1$ , the transfer matrix  $T_{zw}$  is the connection between robust control and the disturbance attenuation problem in which w stands for the disturbance inputs as shown by (2.14). The  $H_\infty$  control framework includes performance specifications, disturbance rejection, control input limitations, and robustness requirements. In the initial design steps the nominal plant G is obtained from the mathematical models developed in Section III.  $H_\infty$  controller is generated in Matlab using the nominal plant G and weights  $W1$  and  $W3$  ensuring the performance and stability requirements [6]. Using the Matlab Robust Control Toolbox the controller K is obtained by the 'mixsyn' function as follows:

$$[K,CL,GAM]=mixsyn (G,W1,W2,W3);$$

where K is the controller CL is the close loop for the system and  $GAM = \gamma$  as shown in (5.1).

Fig. 5.1 shows the linearized ball position generated by the H-infinity controller. The performance and stability bounds offered by the controller are illustrated on Fig. 5.2

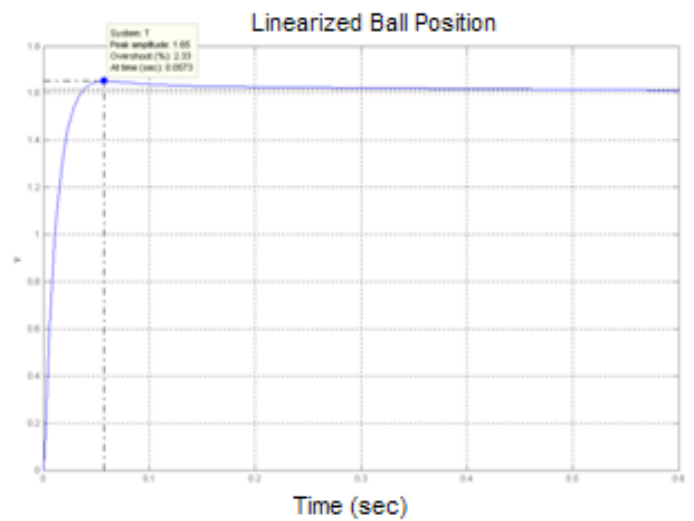


Fig. 5.1: Ball position in the linearized system

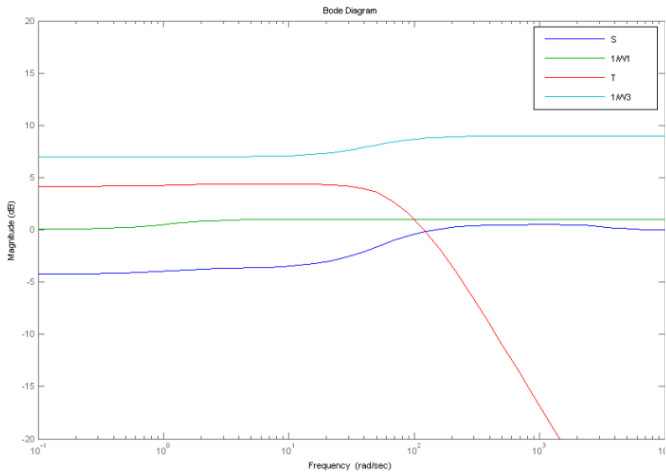


Fig. 5.2: Specification requirements

Simulink diagrams of the Maglev system are derived as per the models of Section III. Figures below also describe the different blocks of the Simulink model:

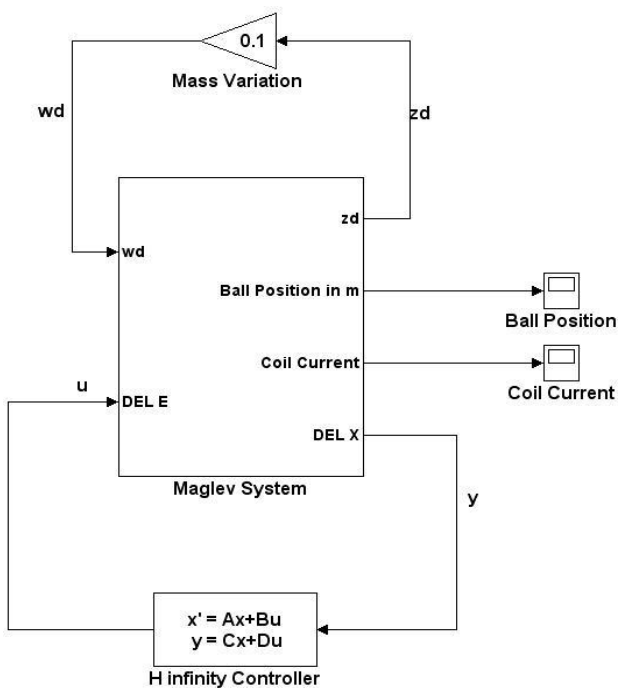


Fig. 5.1: Simulink model of the controlled plant

Fig. 5.1 shows the controlled plant with perturbation.

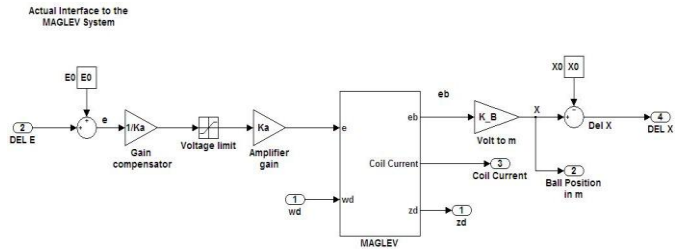


Fig. 5.2: Simulink diagram of a linear maglev model

From the mathematical models of maglev system described in section III, simulink blocks for the maglev system are developed and linearized around the equilibrium point as shown in Fig. 5.2 The simulink diagram for the non linear maglev model is also shown on Fig. 5.3

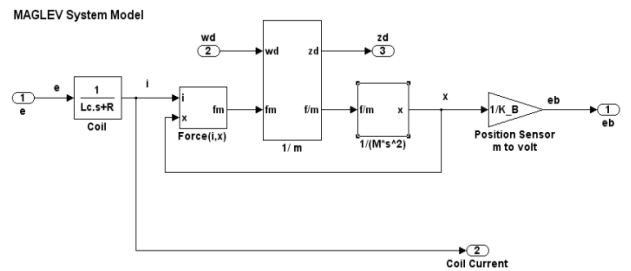


Fig. 5.3: Simulink diagram of non-linear maglev model  
Fig. 5.4 describes the effect of mass variation on the system and the acceleration generated due to the resultant force.

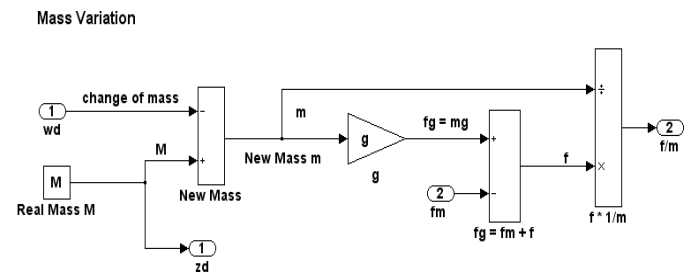


Fig. 5.4: Simulink diagram for mass variation block

Finally, the ball dynamics shown on Fig. 5.5 addresses the steps of getting ball position from its acceleration.

## Ball Dynamics

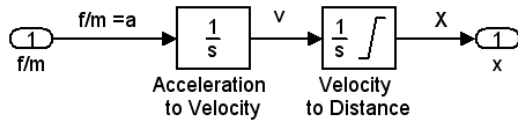


Fig. 5.5: Simulink diagram for ball dynamics block

## VI. SIMULATION RESULT AND ANALYSIS

A complete Simulink model of the controlled plant under perturbation is shown in Fig. 5.1. A variation of 10% mass variation is applied to the simulation and the system output is observed. The controlled ball position and coil current response from the system are shown on Fig. 6.1 and Fig. 6.2 respectively.

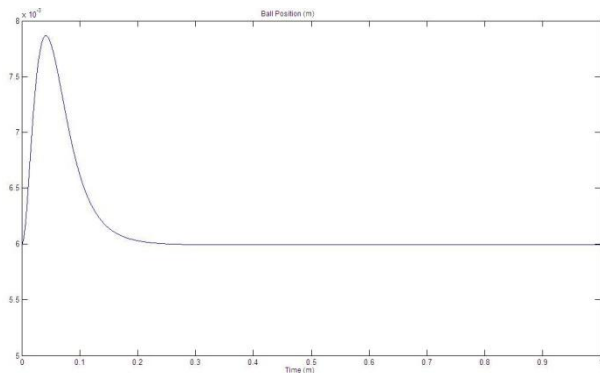


Fig. 6.1: Controlled ball position with 10% variation of mass

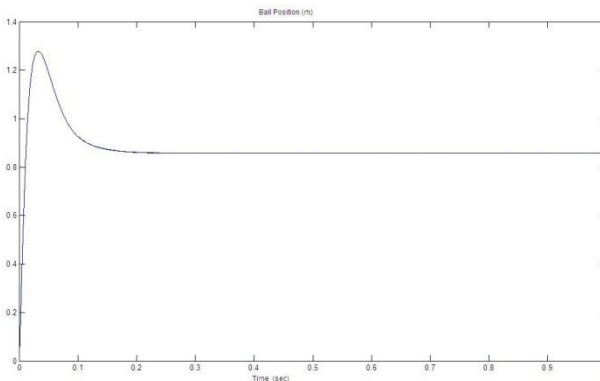


Fig. 6.1: Coil current response at equilibrium under 10% variation of mass

When the ball was placed close to the equilibrium point the controller produced an appropriate action that was fast enough to avoid large deviations of the steel ball position. Even under slight change of mass the controller drove the ball to the equilibrium position and ensured the performance and stability condition as described by (2.3) and (2.11).

## VII. CONCLUSION

H-infinity loop shaping method is used for the design of the controller. Detailed mathematical models and design steps are addressed in this paper. The controller meets the requirements for its robust performance and stability. The simulation results show the controller works perfectly when the ball is placed close to the equilibrium point. In order to cope with a real system or the test-bed, the controller needs some improvements, especially on the weights.

## REFERENCES

- [1] V. A. Oliveira, E. F. Costa, and J. B. Vargas, "Digital implementation of a magnetic suspension control system for laboratory experiments," *IEEE Trans. Educ.*, vol. 42, no. 4, pp. 315–322, Nov. 1999
- [2] V. A. Oliveira, E. S. Tognetti and Daniel Siqueira, "Robust controllers enhanced with design and implementation processes," *IEEE Trans. Educ.*, vol. 49, no. 3, Aug. 2006
- [3] Sigurd Skogestad and Ian Postlethwaite, 'Multivariable Feedback Control Analysis and Design' John Wiley Sons, Chichester, New York, 2005
- [4] K. Zhou, *Essentials of Robust Control*. Upper Saddle River, NJ: Prentice- Hall, 1998.
- [5] T. H. Wong, "Design of a magnetic levitation control system—An undergraduate project," *IEEE Trans. Educ.*, vol. 29, no. 4, pp. 196–200, Nov. 1986.
- [6] R. Y. Chiang and M. G. Safonov, *Robust Control Toolbox User Guide*. Natick, MA: The MathWorks, Inc., 1996.
- [7] *Magnetic Levitation Plant Manual*, Quanser Inc. Markham, Ontario, Canada